Colloid Polym Sci 280: 234–244 (2002)
© Springer-Verlag 2002

ORIGINAL CONTRIBUTION

Chin-Ping Yang
Ruei-Shin Chen
Mao-Feng Hsu

Organosoluble optically transparent poly(amide-imide)s based on 2,2-bis[*N*-(3-carboxyphenyl)phthalimidyl]-hexafluoropropane and 2,2-bis[*N*-(4-carboxyphenyl)phthalimidyl]-hexafluoropropane and various aromatic diamines

Received: 25 April 2001
Accepted: 27 June 2001

C.-P. Yang (✉) · R.-S. Chen · M.-F. Hsu
Department of Chemical Engineering
Tatung University, 40 Chungshan North
Road, Section 3, Taipei 104, Taiwan
e-mail: cpyang@ttu.edu.tw
Tel.: +886-2-25925252 ext. 2977
Fax: +886-2-25861939

Abstract Two diimide-dicarboxylic acids, 2,2-bis[*N*-(4-carboxyphenyl)phthalimidyl]hexafluoropropane (*p*-I) and 2,2,-bis[*N*-(3-carboxyphenyl)phthalimidyl]hexafluoropropane (*m*-I), were prepared by azeotropic condensation of 4,4′-(hexafluoroisopropylidene)diphthalic anhydride and *p*-aminobenzoic acid or *m*-aminobenzoic acid at a 1:2 molar ratio in *N*,*N*-dimethylacetamide/toluene. Two series of organosoluble and colorless poly(amide–imide)s were synthesized from diimide–diacid *p*-I or *m*-I with ten kinds of aromatic diamines by direct polycondensation using triphenyl phosphite and pyridine as condensing agents. The thin films cast from *N*,*N*-dimethylacetamide were measured by UV–vis spectroscopy and Macbeth color-eye colorimetery, the cutoff wavelengths of almost all the films were below 400 nm (361–389 nm) and the values of the parameter b^* were between 15.31 and 34.72; these polymers are much lighter in color than other analogous polymers. Almost all the polymer were soluble in *N*-methyl-2-pyrrolodone, *N*,*N*-dimethylacetamide, *N*,*N*-dimethylformamide and dimethyl sulfoxide, and some polymers could dissolve in less polar solvents, such as dioxane and tetrahydrofuran, etc. The cast films exhibited yield strengths of 95–131 MPa, tensile strengths ranging from 92 to 130 MPa, elongations at break from 9 to 27%, and initial moduli from 2.1 to 3.3 GPa. The poly(amide–imide)s had glass-transition temperatures between 259 and 328°C and 10%-weight-loss temperatures above 510 °C in nitrogen and air, indicating excellent thermal stability.

Keywords 2,2-Bis[*N*-(4-carboxyphenyl)phthalimidyl]-hexafluoropropane · 2,2,-Bis[*N*-(3-carboxyphenyl)phthalimidyl]-hexafluoropropane · Colorless · Poly(amide-imide)s · Organosoluble

Introduction

Aromatic polyimides are well known as polymer materials of high performance for their excellent thermal stabilities and balanced mechanical and electric properties [1–7]. They are mainly used in the aerospace and electronic industries in the forms of films and moldings. Optical transparency of polyimide films is of special importance in some applications [8–11]. However, wholly aromatic polyimides strongly absorb in the visible region of the UV–vis spectrum and are pale yellow or deep reddish-yellow; besides, they are difficult to process because of high softening temperatures and limited solubility in commercially available solvents.

In order to increase the optical application of polyimides, a number of very lightly colored to colorless, transparent polyimide films have been synthesized and characterized. Rogers [12] first reported that optically transparent and colorless polyimides can be synthesized from a dianhydride and a diamine that have hexafluoroisopropylidene [$-C(CF_3)_2-$] groups. Dine-Hart and Wright [13] have shown the formation of a charge-transfer complex between alternating electron-donor (diamine) and electron-acceptor (dianhydride) moieties. A lowering of the charge-transfer complexing generally affords polyimides with lighter color. St. Clair and coworkers [14, 15] demonstrated that polyimides containing the hexafluoroisopropylidene group and/or sulfone linkages exhibit high transparency in the visible region. For increasing processability of polyimides, various copolymers have been developed and reported, among them being poly(amide–imide), whose amide groups can improve the solubilities [16, 17]. Furthermore, poly(amide–imide)s are lighter in color than corresponding polyimides.

Among the poly(amide–imide)s, the most common are of the trimellitimide series [18–22], which always show considerable coloration ranging from pale yellow to deep brown; however, we also found that very light colored poly(amide–imide)s can be obtained by using aromatic diamines with terminal meta structures, connected to the amide groups of the poly(amide–imide)s [23, 24]. Reports of poly(amide–imide)s synthesized from dianhydrides, aromatic aminoacids and diamines are fewer than those of the trimellitimide series. The main reason is that except with dianhydride by using 4,4′-(hexafluoroisopropylidene)diphthalic anhydride (6FDA) [25–30], the other dianhydrides do not synthesize soluble poly(amide–imide)s easily. Bruma and coworkers [25, 26], Irvine and coworkers [27, 28] and Manciuc et al. [29] first synthesized diimide–diacid chloride from 6FDA and aminobenzoic acid (ABA) through diimide–diacid (DIDA), and then reacted it with various diamines by low temperature polycondensation to prepare poly(amide–imide)s. Liaw et al. [30] also synthesized poly(amide–imide)s from DIDA and diamines with many kinds of easily soluble groups.

Because the light-colored polyimide and poly(amide–imide) have attracted much attention recently and coloration of DIDA-derived poly(amide-imide)s has not been reported, we synthesized 20 DIDA-derived poly(amide–imide)s by direct polycondensation. Two kinds of DIDA prepared from 6FDA with *p*-ABA or *m*-ABA can easily form soluble poly(amide–imide)s with rigid diamines such as *p*-phenylenediamine and benzidine etc; besides, they can form very light colored (colorless) poly(amide–imide) films with most aromatic diamines. Among these poly(amide–imide)s, 12 polymers have not yet been found before, and the color measurements are all new data.

Experimental

Materials

p-Phenylenediamine (**II**$_a$, from Wako) and benzidine (**II**$_b$, from TCI) were vacuum-distilled before use. All other diamines, such as 4,4′-oxydianiline (**II**$_c$, from Wakayama), 4,4′-diaminobenzanilide (**II**$_d$, from TCI), 1,4-bis(4-aminophenoxy)benzene (**II**$_e$, from TCI) and 4,4′-bis(4-aminophenoxy)biphenyl (**II**$_h$, from TCI), were used as received. The diamines 1,3-bis(4-aminophenoxy)benzene (**II**$_f$), 2,2-bis[4-(4-aminophenoxy)phenyl]propane (**II**$_i$) and 2,2-bis[4-(4-aminophenoxy)phenyl]hexafluoropropane (**II**$_j$) were obtained from Chriskev Corporation and were used without previous purification. 1,2-Bis(4-aminophenoxy)benzene (**II**$_g$) was prepared according to the method reported previously [31]. *p*-ABA (from TCI), *m*-ABA (from TCI) and triphenyl phosphite (TPP, from TCI) were used as received. 6FDA (from Hoechst) was recrystallized from acetic anhydride before use. Commercially available calcium chloride was dried under vacuum at 150 °C for 6 h. *N*-Methyl-2-pyrrolidone (NMP, from Fluka), *N,N*-dimethylacetamide (DMAc, from Fluka), *N,N*-dimethylformamide (DMF, from Fluka) and pyridine (Py, from Wako) were purified by distillation under reduced pressure over calcium hydride and stored over 4-Å molecular sieves.

Synthesis of diimide–dicarboxylic acid

p-ABA (8.22 g, 60 mmol) was dissolved in 45 ml dried DMAc in a 150-ml flask. After the *p*-ABA had dissolved completely, 13.32 g (30 mmol) 6FDA was added to it in one portion. The mixture was stirred at room temperature for 1 h. Toluene (20 ml) was then added, and the mixture was heated at reflux for about 3 h until about 1.08 ml water had distilled off azeotropically in a Dean–Stark trap. Heating was continued to distill off the residual toluene. After cooling, methanol was added and the precipitated product

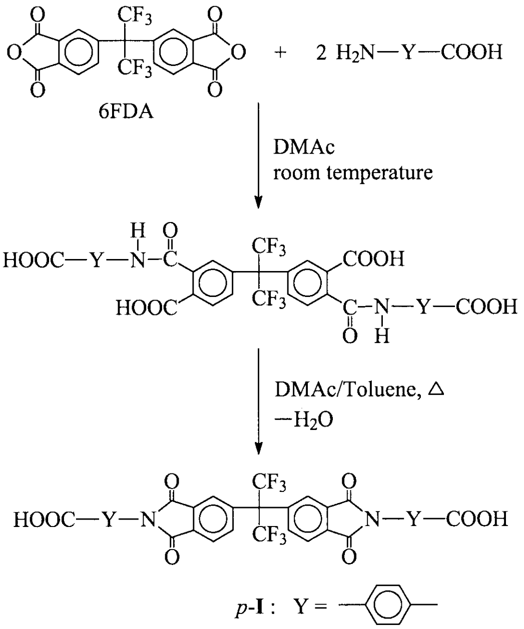

Scheme 1

was isolated by filtration, purified by recrystallization from DMF–methanol solution and dried in a vacuum to give 19.38 g DIDA (*p*-**I**) (95% yield).

p-**I** (Scheme 1): m.p. 374 °C. IR (KBr): 2,500–3,500 (acid -OH), 1,791 (imide, symmetric C=O stretching), 1,729 (acid C=O stretching and asymmetric imide C=O stretching), 1,257 (ether C–O–C), 1,382, 1,105, 721 cm^{-1} (imide, imide ring vibration, axial, transverse and out of plane).

^{1}H NMR (400 MHz, DMSO-d_6, δ): 8.22, 8.20 (2H, H_c), 8.12, 8.10 (4H, H_d), 8.00, 7.98 (2H, H_b), 7.79 (2H, H_a), 7.63, 7.61 ppm (4H, H_e) (Fig. 1).

^{13}C NMR (100 MHz, DMSO-d_6, δ): 168.35 (C^{1}), 167.44, 167.31 (C^{2}, C$^{2'}$), 138.75 (C^{5}), 137.21 (C^{12}), 136.83 (C^{3}), 134.19 (C^{6}), 133.78 (C^{8}), 131.53 (C^{7}), 131.12 (C^{10}), 128.81, 125.91, 123.02, 120.13 (C^{13}), 128.27 (C^{11}), 125.63 (C^{4}), 124.86 (C^{9}), 65.25, 65.00, 64.74 ppm (C^{14}) (Fig. 2).

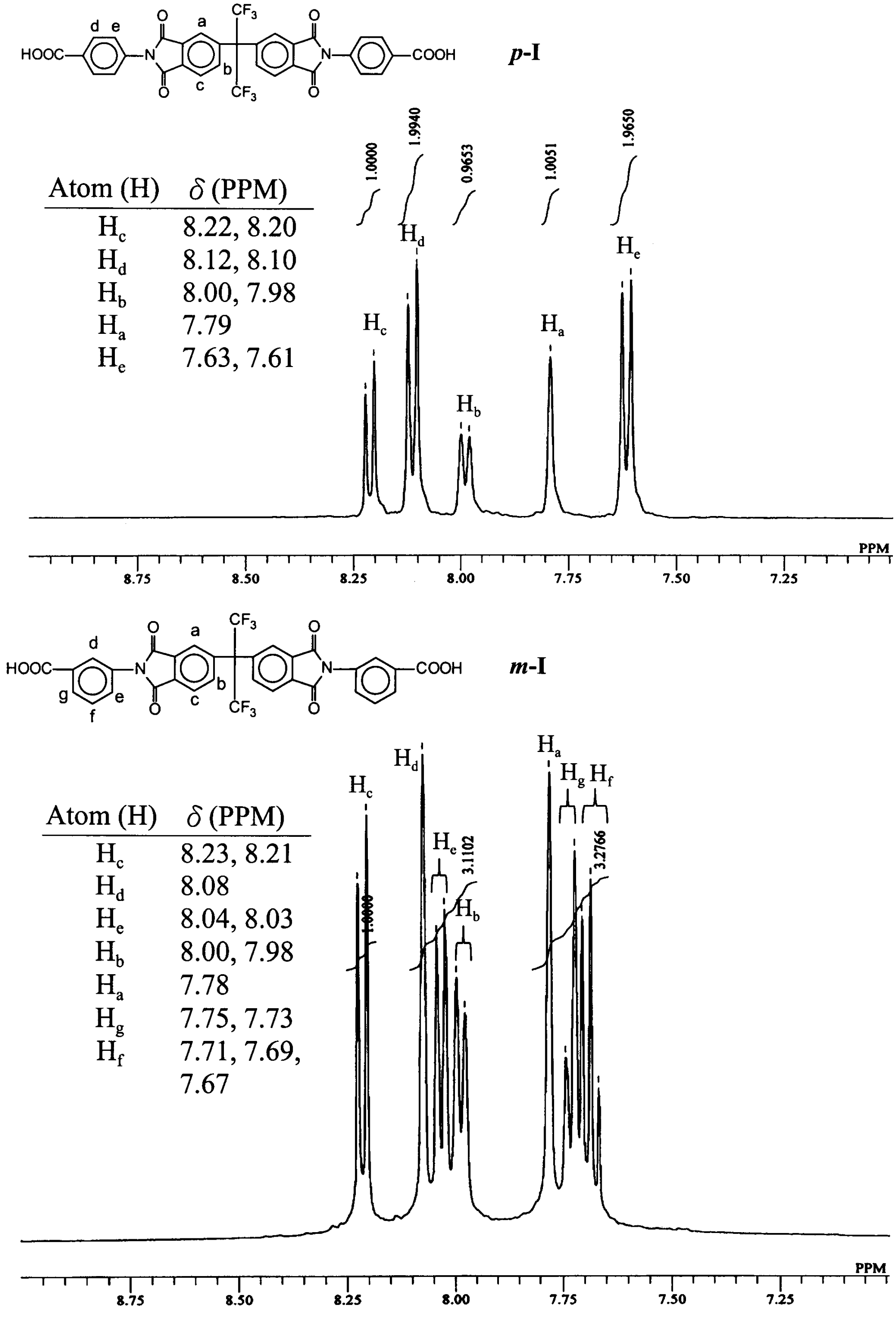

Atom (H)	δ (PPM)
H_c	8.22, 8.20
H_d	8.12, 8.10
H_b	8.00, 7.98
H_a	7.79
H_e	7.63, 7.61

Atom (H)	δ (PPM)
H_c	8.23, 8.21
H_d	8.08
H_e	8.04, 8.03
H_b	8.00, 7.98
H_a	7.78
H_g	7.75, 7.73
H_f	7.71, 7.69, 7.67

Fig. 1 ^{1}H NMR spectra of diimide–diacids *p*-**I** and *m*-**I** (DMSO-d_6)

Fig. 2 ^{13}C NMR spectra of ***p*-I** and ***m*-I** (DMSO-d_6)

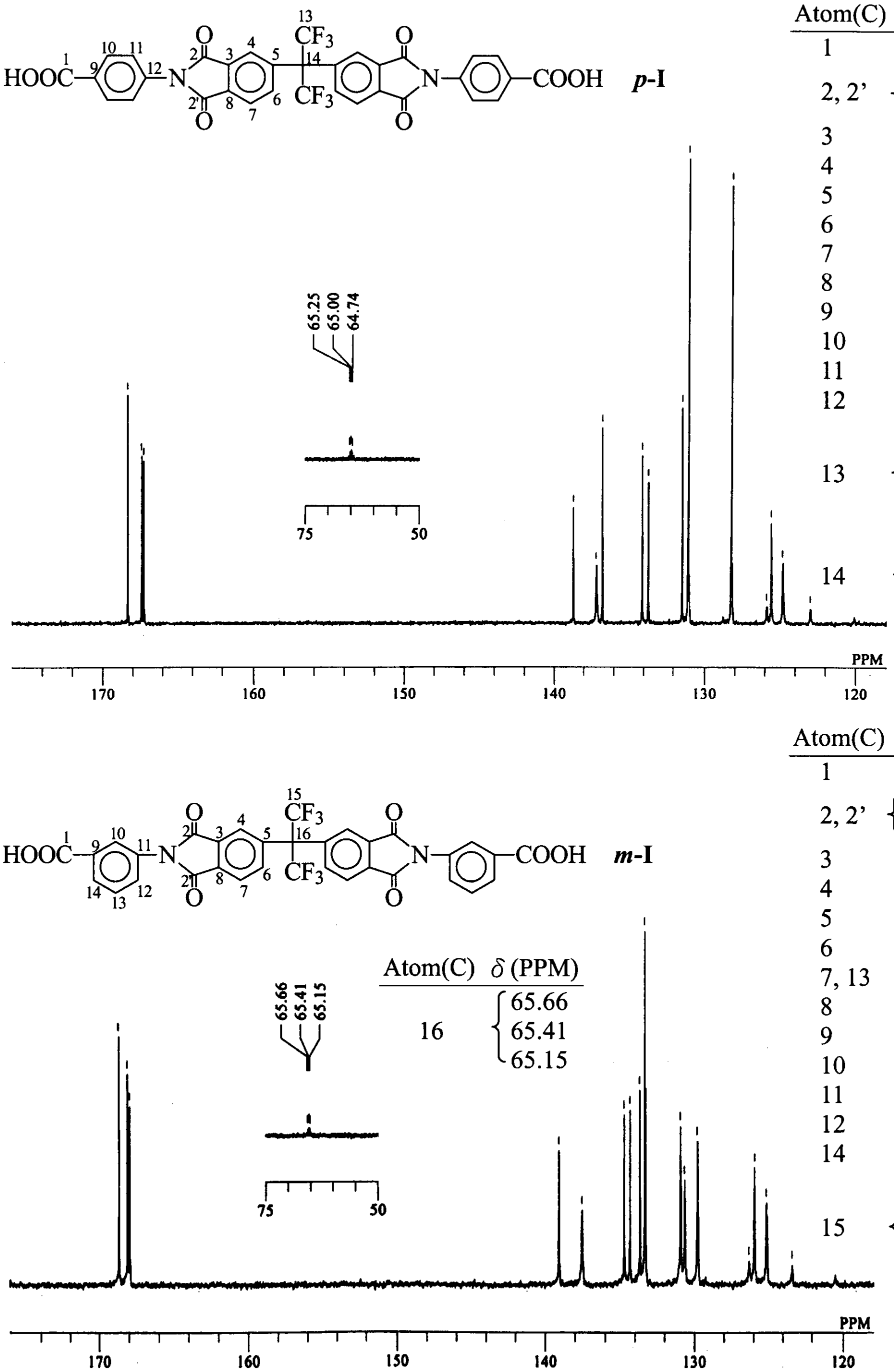

Atom(C)	δ (PPM)
1	168.35
2, 2'	167.44 167.31
3	136.83
4	125.63
5	138.75
6	134.19
7	131.53
8	133.78
9	124.86
10	131.12
11	128.27
12	137.21
13	128.81 125.91 123.02 120.13
14	65.25 65.00 64.74

Atom(C)	δ (PPM)
16	65.66 65.41 65.15

Atom(C)	δ (PPM)
1	168.66
2, 2'	168.09 167.94
3	134.69
4	125.98
5	139.07
6	134.31
7, 13	133.30
8	133.64
9	125.19
10	130.63
11	137.52
12	130.92
14	129.78
15	129.22 126.34 123.44 120.56

Analysis (wt%): calculated for $C_{33}H_{16}N_2O_8F_6$: C, 58.08; H, 2.36; N, 4.10; found: C, 57.90; H, 2.38; N, 4.08.

***m*-I** (Scheme 1) was synthesized in a similar manner. Yield 96%; m.p. 351 °C. IR (KBr): 2,500–3,500 (acid –OH), 1,784 (imide, symmetric C=O stretching), 1,720 (acid C=O stretching and asymmetric imide C=O stretching), 1,261 (ether C–O–C), 1,375, 1,106, 721 cm^{-1} (imide, imide ring vibration, axial, transverse and out of plane).

^{1}H NMR (400 MHz, DMSO-d_6, δ): 8.23, 8.21 (2H, H_c), 8.08 (2H, H_d), 8.04, 8.03 (2H, H_e), 8.00, 7.98 (2H, H_b), 7.78 (2H, H_a), 7.75, 7.73 (2H, H_g), 7.71, 7.69, 7.67 ppm (2H, H_f).

^{13}C NMR (100 MHz, DMSO-d_6, δ): 168.66 (C^1), 168.09, 167.94 (C^2, C$^{2'}$), 139.07 (C^5), 137.52 (C^{11}), 134.69 (C^3), 134.31 (C^6), 133.64 (C^8), 133.30 (C^7, C^{13}), 130.92 (C^{12}), 130.63 (C^{10}), 129.78 (C^{14}), 129.22, 125.34, 123.44, 120.56 (C^{15}), 125.98 (C^4), 125.19 (C^9), 65.66, 65.41, 65.15 ppm (C^{16}).

Analysis (wt%): calculated for $C_{33}H_{16}N_2O_8F_6$: C, 58.08; H, 2.36; N, 4.10; found: C, 57.88; H, 2.37; N, 4.08.

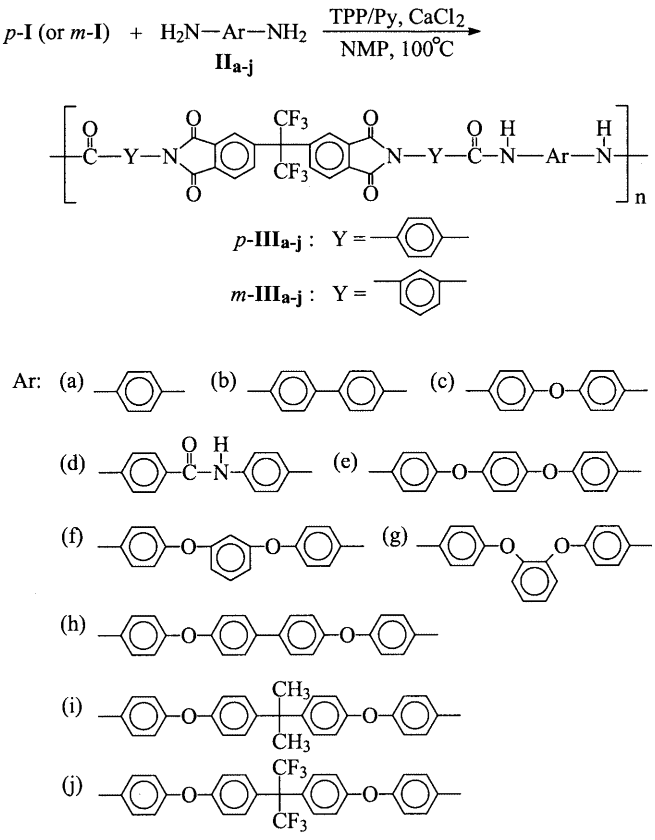

Scheme 2

Synthesis of poly(amide-imide)s

The synthesis of poly(amide–imide) ***p*-III**$_{\mathrm{g}}$ is described as a typical procedure (Scheme 2). A mixture of 0.683 g (1.0 mmol) ***p*-I**, 0.292 g (1.0 mmol) 1,2-bis(4-aminophenoxy)benzene (**II**$_{\mathrm{g}}$), 0.10 g $CaCl_2$, 1.0 ml Py, 0.6 ml TPP and 3.1 ml NMP was heated with stirring at 100 °C for 3 h. The viscosity of the reaction solutions increased after 1 h, and an additional 2.0 ml NMP was added to the reaction mixture. At the end of the reaction, the polymer solution was trickled into stirred methanol, giving rise to a stringy precipitate, which was washed thoroughly with hot water and methanol, collected by filtration and dried. The inherent viscosity of the polymer ***p*-III**$_{\mathrm{g}}$ was 1.16 dl/g at 30 °C, measured at a concentration of 0.5 g/dl in DMAc.

Other poly(amide–imide)s ***p*-III** and ***m*-III** were synthesized in a similar manner. The results of the elemental analysis of the polymers are shown in Table 1.

Measurements

Melting points were measured in capillaries using a Yamato melting point apparatus (model MP-21) without correction. Elemental analyses were obtained using a PerkinElmer model 2400 CHN analyzer. IR spectra were recorded using a Horiba FTIR-720 Fourier transform IR spectrometer. ^{1}H and ^{13}C NMR spectra were determined using a Jeol EX-400 FT-NMR spectrometer. Inherent viscosities of all polymers were determined at 0.5 g/dl concentration using a Cannon–Fenske viscometer at 30 °C. Solubilities were determined at 1% (w/w) concentration. Coloration of the polymers was evaluated using a Macbeth color-eye colorimeter. Measurements were performed with films, using an observational angle of 10° and a Commission International de l'Eclairage (CIE) D illuminant. A CIE LAB color difference equation was used. UV–vis spectra of the polymer films were recorded using a Shimadzu UV-1601 UV–vis recording spectrophotometer at room temperature in air. Differential scanning calorimetery (DSC) traces were measured using TA Instruments DSC 2010 at a rate of 15 °C/min in flowing nitrogen (40 cm^3/min). Thermogravimetric analysis was conducted with a TA Instruments TGA 2050. Experiments were carried out on 10 ± 2-mg samples heated in flowing nitrogen or air (100 cm^3/min) at a heating rate of 20 °C/min. An Instron model 1130 universal tester with a load cell of 5 kg was used to study the stress–strain behavior of the sample. A gauge of 2 cm and a strain rate of 5 cm/min were used for this study. Measurements were performed at room temperature with film specimens (0.5-cm wide, 6-cm long and about 0.05-mm thick), and the average of at least five individual determinations was reported.

Results and discussion

Monomer syntheses

Poly(amide–imide)s ***p*-III**$_{\mathrm{a-j}}$ and ***m*-III**$_{\mathrm{a-j}}$ were synthesized in two steps starting from *p*-ABA or *m*-ABA with 6FDA to prepare diimide–dicarboxylic acids ***p*-I** and ***m*-I**, which were then reacted with various aromatic diamines **II**$_{\mathrm{a-j}}$ by direct polycondensation to prepare poly(amide–imide)s. 2,2-Bis[*N*-(4-carboxyphenyl)phthalimidyl]hexafluoropropane (***p*-I**) and 2,2,-bis[*N*-(3-carboxyphenyl)phthalimidyl]hexafluoropropane (***m*-I**), the new polymer-forming DIDAs with preformed imide rings, were synthesized via the two-stage procedure that included the ring-opening addition of 6FDA with two equivalent amount of *p*-ABA or *m*-ABA at room temperature in polar solvents (such as NMP or DMAc) to form the amide–amide intermediate, followed by thermal cyclodehydration to the diacids ***p*-I** and ***m*-I** at reflux temperature by toluene–water azeotropic distillation, as shown in Scheme 1. The crude ***p*-I** and ***m*-I** were purified by recrystallization from DMF–methanol. The structures of monomers ***p*-I** and ***m*-I** were confirmed by elemental analysis and IR, ^{1}H NMR and ^{13}C NMR spectroscopy.

The ^{1}H and ^{13}C NMR spectra of diacids ***p*-I** and ***m*-I** are shown in Figs. 1 and 2. The ^{1}H NMR spectrum of ***p*-I** showed five main signals because of different environments of the protons. The H_c and H_d close to the imide ring and carboxylic acid (ortho-oriented protons) appeared in the downfield region of the spectrum, owing to the resonance and inductive effect; the H_a and H_b ortho-oriented to the hexafluoroisopropylidene group shifted to the upfield region, owing to the shielding effect. The ^{13}C NMR spectrum revealed 20 signals, which were in agreement with the predicted structure of ***p*-I**. Carbons C^1, C^2 and $C^{2'}$ of the carbonyl groups were evidenced in the downfield region at 167.31–168.35 ppm, and the different shifts of C^2 and $C^{2'}$ were caused by the different distance to the $–C(CF_3)_2–$ group. Owing to the fluorine atoms of $–CF_3$, the C^{13} signal was split and formed a

Table 1 Synthesis and elemental analysis of poly(amide–imide)s. The polymerization was carried out with 1 mmol of each monomer, 5–6 ml *N*-methyl-2-pyrrolodone (*NMP*), 0.1–0.15 g $CaCl_2$, 0.8–1.2 ml pyridine (*Py*) and 0.6 ml triphenyl phosphite at 100 °C for 3 h

Polymer	η_{inh}[a] (dl/g)	Formula (molecular weight)		Elemental analysis (%)[b]			Moisture uptake (%)[c]
				C	H	N	
p-III$_\mathrm{a}$	0.78	$(C_{39}H_{20}N_4O_6F_6)_n$	Calc	62.08	2.67	7.42	1.35
		$(754.69)_n$	Found	59.57	3.14	7.32	
			Corrected	60.37	3.10	7.41	
p-III$_\mathrm{b}$	0.80	$(C_{45}H_{24}N_4O_6F_6)_n$	Calc	65.05	2.91	6.75	4.27
		$(830.70)_n$	Found	62.30	3.27	6.38	
			Corrected	64.93	3.15	6.65	
p-III$_\mathrm{c}$	1.04	$(C_{45}H_{24}N_4O_7F_6)_n$	Calc	63.82	2.86	6.62	3.75
		$(846.70)_n$	Found	61.43	3.12	6.29	
			Corrected	63.73	3.00	6.53	
p-III$_\mathrm{d}$	0.64	$(C_{46}H_{25}N_5O_7F_6)_n$	Calc	63.24	2.88	8.02	4.59
		$(873.72)_n$	Found	60.34	3.28	7.56	
			Corrected	63.11	3.13	7.91	
p-III$_\mathrm{e}$	0.93	$(C_{51}H_{28}N_4O_8F_6)_n$	Calc	65.25	3.01	5.97	0.84
		$(938.80)_n$	Found	63.46	3.28	5.92	
			Corrected	63.99	3.25	5.96	
p-III$_\mathrm{f}$	1.10	$(C_{51}H_{28}N_4O_8F_6)_n$	Calc	65.25	3.01	5.97	2.26
		$(938.80)_n$	Found	63.58	3.73	5.59	
			Corrected	65.02	3.65	5.72	
p-III$_\mathrm{g}$	1.16	$(C_{51}H_{28}N_4O_8F_6)_n$	Calc	65.25	3.01	5.97	3.14
		$(938.80)_n$	Found	63.20	3.24	5.62	
			Corrected	65.18	3.14	5.80	
p-III$_\mathrm{h}$	1.06	$(C_{57}H_{32}N_4O_8F_6)_n$	Calc	67.46	3.18	5.52	2.82
		$(1014.89)_n$	Found	65.56	3.42	5.23	
			Corrected	67.41	3.32	5.38	
p-III$_\mathrm{i}$	0.82	$(C_{60}H_{38}N_4O_8F_6)_n$	Calc	68.18	3.62	5.30	2.40
		$(1056.26)_n$	Found	66.54	3.78	4.97	
			Corrected	68.14	3.69	5.09	
p-III$_\mathrm{j}$	0.98	$(C_{60}H_{32}N_4O_8F_{12})_n$	Calc	61.84	2.77	4.81	1.78
		$(1164.92)_n$	Found	60.74	3.17	4.52	
			Corrected	61.82	3.11	4.60	
m-III$_\mathrm{a}$	0.73	$(C_{39}H_{20}N_4O_6F_6)_n$	Calc	62.08	2.67	7.42	3.06
		$(754.69)_n$	Found	60.18	2.99	6.98	
			Corrected	62.02	2.90	7.19	
m-III$_\mathrm{b}$	0.89	$(C_{45}H_{24}N_4O_6F_6)_n$	Calc	65.05	2.91	6.75	0.89
		$(830.70)_n$	Found	62.71	3.11	6.69	
			Corrected	63.27	3.08	6.74	
m-III$_\mathrm{c}$	0.85	$(C_{45}H_{24}N_4O_7F_6)_\mathrm{n}$	Calc	63.82	2.86	6.62	0.30
		$(846.70)_n$	Found	61.46	3.34	6.64	
			Corrected	61.64	3.33	6.66	
m-III$_\mathrm{d}$	0.79	$(C_{46}H_{25}N_5O_7F_6)_n$	Calc	63.24	2.88	8.02	0.87
		$(873.72)_n$	Found	60.43	3.23	7.95	
			Corrected	60.96	3.20	8.01	
m-III$_\mathrm{e}$	0.99	$(C_{51}H_{28}N_4O_8F_6)_n$	Calc	65.25	3.01	5.97	1.84
		$(938.80)_n$	Found	63.02	3.23	6.08	
			Corrected	64.18	3.17	6.19	
m-III$_\mathrm{f}$	0.76	$(C_{51}H_{28}N_4O_8F_6)_n$	Calc	65.25	3.01	5.97	1.68
		$(938.80)_n$	Found	63.19	3.19	6.07	
			Corrected	64.25	3.14	6.17	
m-III$_\mathrm{g}$	0.83	$(C_{51}H_{28}N_4O_8F_6)_n$	Calc	65.25	3.01	5.97	1.17
		$(938.80)_n$	Found	63.21	3.17	6.04	
			Corrected	63.95	3.13	6.11	
m-III$_\mathrm{h}$	0.85	$(C_{57}H_{32}N_4O_8F_6)_n$	Calc	67.46	3.18	5.52	3.11
		$(1014.89)_n$	Found	65.36	3.36	5.72	
			Corrected	67.39	3.26	5.90	
m-III$_\mathrm{i}$	0.50	$(C_{60}H_{38}N_4O_8F_6)_\mathrm{n}$	Calc	68.18	3.62	5.30	2.70
		$(1056.26)_n$	Found	66.34	3.83	5.03	
			Corrected	68.13	3.73	5.17	

Table 1 (Contd.)

Polymer	$\eta_{\text{inh}}{}^{a}$ (dl/g)	Formula (molecular weight)		Elemental analysis (%)[b]			Moisture uptake (%)[c]
				C	H	N	
***m*-III$_j$**	0.50	$(C_{60}H_{32}N_4O_8F_{12})_n$	Calc	61.84	2.77	4.81	1.46
		$(1164.92)_n$	Found	60.94	2.96	4.60	
			Corrected	61.83	2.92	4.67	

[a] Measured at a polymer concentration of 0.5 g/dl in *N*,*N*-dimethylacetamide at 30 °C

[b] For C and N: corrected value = found value × (100% + moisture uptake percentage). For H: corrected value = found value × (100%– moisture uptake percentage)

[c] Moisture uptake (%) = $(W-W_0)/W_0 \times 100\%$; W is the weight of the polymer sample after standing at room temperature and W_0 is the weight of the polymer sample after being dried in a vacuum at 100 °C for 10 h

quartet (128.81, 125.91, 123.02 and 120.13 ppm, coupling constant $J = 290$ Hz). Because the structures of ***p*-I** and ***m*-I** are similar, the signals can be compared for the relative position in the NMR spectra. The signals of protons H_a, H_b, H_c and H_d of ***m*-I** appeared at almost the same positions in the spectrum of ***p*-I**. For the rest of the protons of ***m*-I**, H_e was located at the ortho position of the imide ring, so the signal of H_e appeared at a lower field than those of H_f and H_g, owing to the resonance. The H_g signal appeared at a lower upfield region than that of H_f, because H_g was affected by the inductive effect of the carboxyl group. In the ^{13}C NMR spectrum of ***m*-I**, C^7 and C^{13} overlapped owing to similar environments, and the shifts for most carbons were almost the same as those of ***p*-I**, in agreement with the proposed structure.

Polymer syntheses

Two series of poly(amide-imide)s were synthesized by a phosphorylation reaction using TPP as a promoter in NMP in the presence of Py and $CaCl_2$ (Scheme 2). The results of the polycondensation are summarized in Table 1. All the polymerizations proceeded homogeneously throughout the reaction. The viscosity of the reaction solutions increased after about 1 h, and an additional volume of NMP was added to the reaction mixture to reduce the viscosity of the polymer solution for smooth stirring. The formation of poly(amide–imide)s was confirmed by IR spectroscopy and elemental analysis. The typical IR spectra of polymers ***p*-III$_c$** and ***m*-III$_c$** (Fig. 3) displayed characteristic absorption bands for the imide ring at about 1,780 and 1,720 cm^{-1} because of the asymmetrical and symmetrical C = O stretching vibration and at about 1,100 and 720 cm^{-1} because of imide ring deformation. The absorptions of the amide groups appeared at about 3,350 and 1,670 cm^{-1}. The results of the elemental analysis of all the poly(amide-imide)s are also listed in Table 1. The uptakes of water were in the range 0.30–4.59%; these were calculated from the weight change of the vacuum-dried polymer samples after they had been exposed to air at room temperature for 8–10 h. When the values were corrected for elimination of the amount of absorbed water, the corrected values were in good agreement with the calculated ones.

Properties of polymers

The qualitative solubilities of these two series of poly(amide–imide)s are summarized in Table 2. Among these poly(amide–imide)s, the diamines used were relatively rigid (e.g. **II$_{a,b,c,e,h}$**), but the polymers formed had

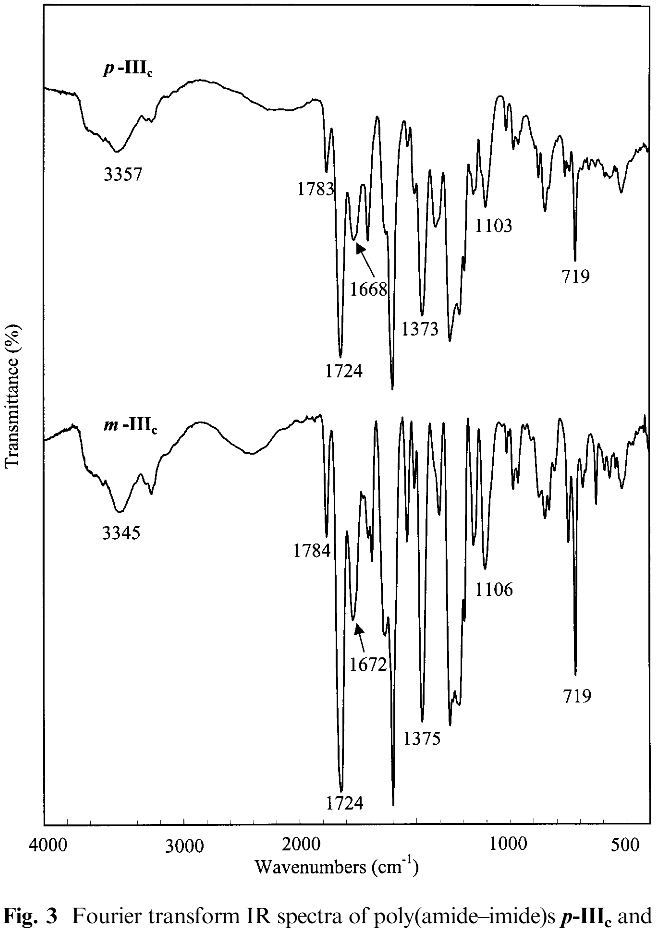

Fig. 3 Fourier transform IR spectra of poly(amide–imide)s ***p*-III$_c$** and ***m*-III$_c$**

Table 2 Solubility of poly(amide–imide)s in various solvents: NMP, *N*,*N*-dimethylacetamide (*DMAc*), *N*,*N*-dimethylformamide (*DMF*), dimethyl sulfoxide (*DMSO*), *m*-cresol, Py, dioxane, tetrahydrofuran (*THF*), H_2SO_4. Solubility: soluble (+), swelling (*S*), partially soluble (±) and insoluble (–)

Polymer	Solvents								
	NMP	DMAc	DMF	DMSO	*m*-Cresol	Py	Dioxane	THF	H_2SO_4
***p*-III**$_a$	+	+	+	+	S	–	–	–	+
***p*-III**$_b$	+	+	+	+	S	–	–	–	+
***p*-III**$_c$	+	+	+	+	+	+	+	+	+
***p*-III**$_d$	+	+	S	+	S	–	–	–	+
***p*-III**$_e$	+	+	+	+	+	+	–	+	+
***p*-III**$_f$	+	+	+	+	+	+	S	+	+
***p*-III**$_g$	+	+	+	+	+	+	S	+	+
***p*-III**$_h$	+	+	+	+	+	+	S	+	+
***p*-III**$_i$	+	+	+	+	+	+	+	+	+
***p*-III**$_j$	+	+	+	+	+	+	+	+	+
***m*-III**$_a$	+	+	+	+	+	+	–	+	+
***m*-III**$_b$	+	+	+	+	+	+	S	±	+
***m*-III**$_c$	+	+	+	+	+	+	S	+	+
***m*-III**$_d$	+	+	+	+	+	+	S	S	+
***m*-III**$_e$	+	+	+	+	+	+	±	+	+
***m*-III**$_f$	+	+	+	+	+	+	+	+	+
***m*-III**$_g$	+	+	+	+	+	+	+	+	+
***m*-III**$_h$	+	+	+	+	+	+	+	+	+
***m*-III**$_i$	+	+	+	+	+	+	+	+	+
***m*-III**$_j$	+	+	+	+	+	+	+	+	+

good solubilities in organic solvents. Poly(amide–imide)s ***p*-III** were all soluble in aprotic polar solvents such as NMP, DMAc, DMF and DMSO, and most of them were also soluble in less polar solvents, such as *m*-cresol, pyridine, dioxane and THF. ***p*-III**$_a$ and ***p*-III**$_b$ were both insoluble in less polar solvents, because their diamine moieties were stiff, which resulted in a lower percentage of flexible group in the main chain. ***p*-III**$_d$ was also insoluble in less polar solvents owing to higher percentages of amide groups in backbone; these formed more intermolecular hydrogen bonds. In comparison with series ***p*-III**, series ***m*-III** showed better solubility in various solvents.

Two series polymers had better solubilities than the typical poly(amide–imide)s derived from trimellitic anhydride, and were all readily soluble in NMP and DMAc without LiCl. This is because the main chain contains the bulky hexafluoroisopropylidene groups so as to produce steric hindrance, which prevents close chain-packing and allows solvent molecules to diffuse into the polymer chains. Poly(amide–imide)s ***m*-III** had better solubilities than poly(amide–imide)s ***p*-III** because the former had more *m*-phenylene linkages (*m*-ABA), such that the rigidity of the polymers decreased greatly, which resulted in an increased free volume between the polymer chains and decreased intermolecular interactions.

The coloration of the polymers was elucidated from the yellowness or redness indices observed with a Macbeth color-eye colorimeter, and the CIE LAB color system was applied. The color coordinates of poly(amide–imide)s ***p*-III**, ***m*-III** and the corresponding polymers **IV–IX** (Scheme 3) are given in Table 3. The cutoff wavelengths of the polymers are recorded from the transmission UV–vis spectra. The paper referred to in Table 3 was the result of white paper that was used as a standard. When the polymer films were tested, a white paper was placed behind the films as a background. For colorless film, the values of a^* and b^* are 0 and the value of L^* is 100. In general, coloration of aromatic polymer is due to their conjugated aromatic structures and/or the intermolecular and intramolecular charge-transfer complex (CTC) formation. From a previous report [32], lighter color polymer films are achieved when the polymer contains more *m*-phenylene or $-C(CF_3)_2-$ groups, because *m*-phenylene and electron-withdrawing

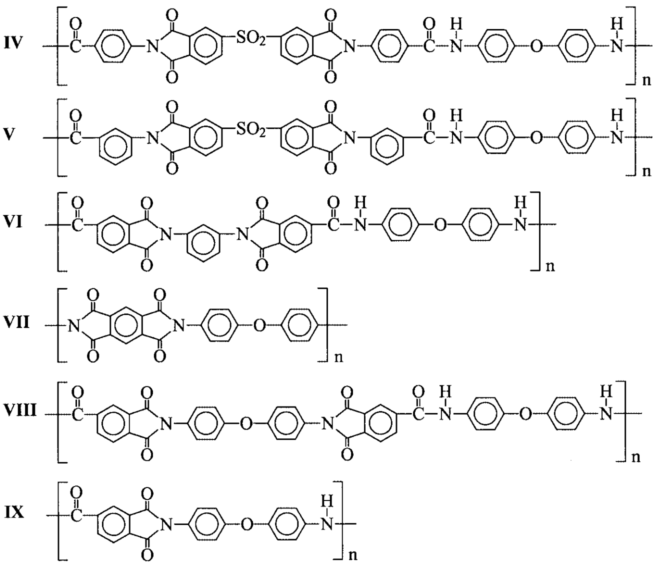

Scheme 3

–C(CF$_3$)$_2$– can decrease the extent of conjugation and CTC. Therefore, both series of poly(amide–imide)s synthesized in this study had a lighter color than common polyimides or poly(amide–imide)s.

The changes in the a^* and L^* values of series **p-III** and **m-III** were small, but those of the b^* values (a yellowness index) were large. On comparing the b^* values of polymers **p-III** with their analogous **m-III**, the **m-III** polymers contained more meta-linked phenylene groups in the polymer chain, so the b^* values of polymers **m-III** were smaller than those of the corresponding polymers **p-III**. The smallest b^* values of **p-III$_j$** and **m-III$_j$** in the two series were due to higher percentages of –C(CF$_3$)$_2$– groups in the polymer chain. Poly(amide–imide)s **p-III$_b$** and **m-III$_b$** using benzidine as a diamine monomer had the largest b^* values in the two series, indicating that polymers containing biphenyl moieties in the main chain would have stronger color intensity. The results shown in Table 3 indicate that two series of poly(amide–imide)s showed a smaller b^* value by contrast with the corresponding **IV–IX** series polymers. Although the **VI** poly(amide–imide) had a *m*-phenylene group between two imide rings in the polymer chain, this arrangement was not effective in reducing the color; so the **VI** polymer showed a larger b^* value than the other series and a b^* value of up to 73.59. The b^* values of the **VII**, **VIII** and **IX** were also large, indicating intense color of these polymer types. **p-III$_c$** and **m-III$_c$** showed smaller b^* values than **IV** and **V**, and this may be due to the –C(CF$_3$)$_2$– groups being more effective than sulfone groups in reducing color.

Table 3 Color coordinates of poly(amide-imide)s. The color parameters were calculated according to a CIE LAB equation, using paper as a standard. L^* is lightness; 100 means white, while 0 implies black. A positive a^* means a red color, while a negative a^* indicates a green color. A positive b^* means a yellow color, while a negative b^* implies a blue color

Polymer	L^*	a^*	b^*	Cutoff wavelength (nm)	Film thickness (μm)
Paper	92.73	−0.34	0.20		
p-III$_a$	89.53	−4.62	34.72	385	40
p-III$_b$	80.57	−0.74	52.25	415	63
p-III$_c$	90.61	−5.13	31.71	381	46
p-III$_d$	84.39	−0.38	32.33	401	67
p-III$_e$	87.26	−4.51	25.93	384	53
p-III$_f$	87.21	−4.52	19.98	378	52
p-III$_g$	88.31	−4.08	24.34	381	53
p-III$_h$	85.17	−4.28	33.10	385	53
p-III$_i$	86.68	−3.08	31.87	380	53
p-III$_j$	89.55	−4.09	19.90	373	56
m-III$_a$	85.93	−4.40	29.45	383	50
m-III$_b$	83.18	−3.28	49.28	404	60
m-III$_c$	87.16	−4.33	30.56	381	72
m-III$_d$	88.39	−6.57	32.89	389	53
m-III$_e$	88.30	−3.83	24.82	375	60
m-III$_f$	85.27	−3.28	24.65	374	63
m-III$_g$	87.70	−4.30	23.84	371	62
m-III$_h$	85.96	−3.61	29.75	382	55
m-III$_i$	84.90	−2.19	29.70	376	52
m-III$_j$	89.80	−1.77	15.31	361	54
IV	72.64	4.53	36.27	414	53
V	79.48	−1.93	33.04	405	61
VI	78.33	−10.07	73.59	470	64
VII	76.23	10.98	62.88	465	70
VIII	72.07	−0.69	54.01	445	60
IX	69.13	12.44	54.02	429	62

The transmission UV–vis absorption spectra of poly(amide–imide) and polyimide films are showed in Figs. 4 and 5. The spectra of typical polymers **p-III$_g$** and **m-III$_g$** are illustrated in Fig. 4. The **m-III$_g$** film exhibited a cutoff wavelength at 371 nm and were highly transparent and colorless in the range from 370 to 800 nm. In Fig. 5, **m-III$_c$** were fairly transparent and almost colorless in contrast to other polymers. When the dianhydride moieties in **m-III$_c$** were replaced by 3,3′,4,4′-diphenyl-

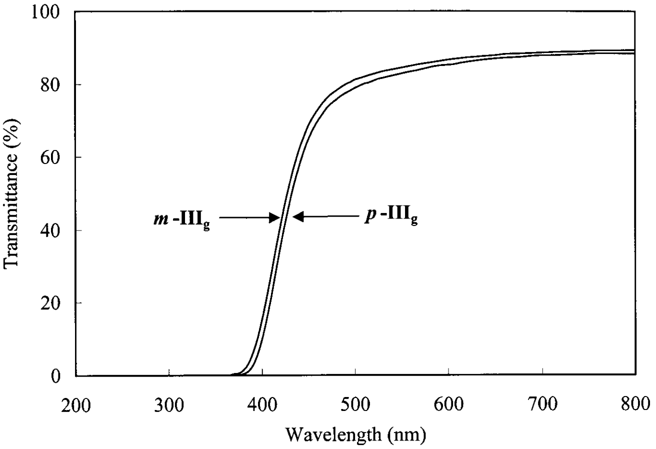

Fig. 4 Transmission UV–vis absorption spectra of poly(amide–imide)s **p-III$_g$** and **m-III$_g$**

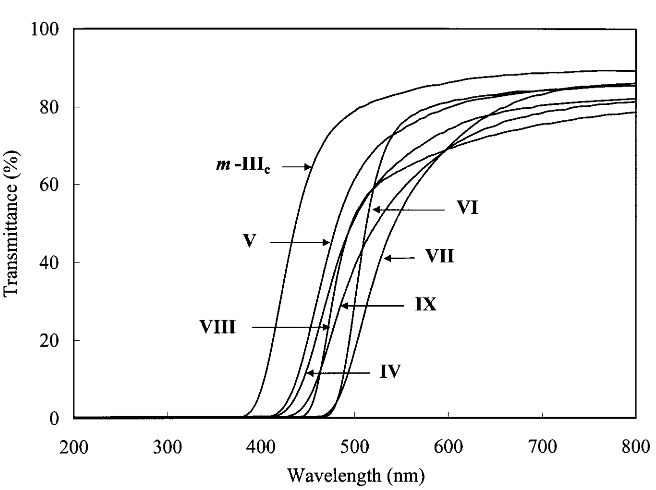

Fig. 5 Transmission UV–vis absorption spectra of poly(amide–imide) and polyimide films

sulfonetetracarboxylic dianhydride (DSDA), the transparency of the UV–vis spectrum (**V**) decreased obviously and the cutoff wavelength shifted to 405 nm. This result reveals that the polymer based on 6FDA had a lighter color than that based on DSDA. The intense color observed for polyimide **VII** (Kapton) is obviously caused by the absorption curve trailing to longer wavelengths (470–700 nm). This is attributed to higher percentage of the imide group and the absence of *m*-phenylene groups in polymer **VII**. The cutoff wavelength of **VII** shifted to 465 nm, revealing the increase in CTC formation by pyromellitic dianhydride. In general, trimellitimide series polymers, such as those synthesized from trimellitic anhydride and 4,4′-oxydianiline, are deep yellow, so polymers ***p*-III** and ***m*-III** are superior to these polymers in optical transparency. For example, ***m*-III**$_{c}$ was lighter colored than analogous poly(amide–imide)s **VI**, **VIII** and **IX**, as shown in Fig. 5.

With the exception of a brittle film of ***p*-III**$_{b,d}$, transparent and tough films could be cast from the DMAc solutions of the rest of the poly(amide–imide)s. The tensile properties are summarized in Table 4. Most of the polymers exhibited yield points on their stress–strain curves, high tensile strength, and moderate elongation at break, indicative of great toughness and a ductile nature. Polymers ***p*-III** exhibited larger elongations at break, but most of the polymers ***m*-III** showed higher tensile strengths. These films had yield strengths of 95–131 MPa, tensile strengths of 92–130 MPa, elongations at break of 9–27%, and initial moduli of 2.1–3.3 GPa. From these results, these poly(amide–imide)s all possessed good tensile properties with strong and tough characters, suggesting that these poly(amide–imide)s can be applied as new materials for engineering plastics.

The thermal properties of all the poly(amide–imide)s were evaluated by thermogravimetry (TG) and DSC. The thermal behavior data of all the polymers are listed in Table 5. Since the residual water or solvent and the history of thermal annealing may sometimes influence the first run of DSC, the samples were at first heated to 400 °C and then quenched to room temperature, and the glass-transition temperatures (T_g) was determined from the subsequent DSC heating trace. The T_g values of poly(amide–imide)s ***p*-III** and ***m*-III** were in the ranges 281–322 and 259–328 °C, respectively, depending on the structure of the diamine component and in the order of increasing stiffness of the polymer backbones. Polymers ***p*-III**$_{a}$ and ***p*-III**$_{b}$ containing no flexible structures in the diamine and ***p*-III**$_{d}$ containing a amide group in the diamine did not exhibit T_g below 400 °C; series ***m*-III**, bearing a less symmetrical *m*-phenylene unit in ***m*-I**, increased the overall flexibility of the polymer chain and, thus, all the polymers exhibited a step transition in the DSC curves. For ***p*-III**$_{h,i,j}$ and ***m*-III**$_{h,i,j}$, ***p*-III**$_{h}$ and ***m*-III**$_{h}$ possessed the highest T_g values owing to the biphenyl structure in the diamine (***p*-III**$_{h}$ > ***p*-III**$_{j}$ > ***p*-III**$_{i}$; ***m*-III**$_{h}$ > ***m*-III**$_{j}$ > ***m*-III**$_{i}$). Diamine **II**$_{i}$ has a structure analogous to **II**$_{j}$, but the substituent magnitude of $-CH_3$

Table 4 Tensile properties of poly(amide–imide) films

Polymer[a]	Yield strength (MPa)	Tensile strength (MPa)	Elongation at break (%)	Tensile modulus (GPa)
***p*-III**$_{a}$	131	130	11	3.3
***p*-III**$_{c}$	111	110	22	2.7
***p*-III**$_{e}$	105	102	20	2.4
***p*-III**$_{f}$	98	93	24	2.4
***p*-III**$_{g}$	100	92	27	2.4
***p*-III**$_{h}$	100	99	23	2.1
***p*-III**$_{i}$	95	94	22	2.2
***p*-III**$_{j}$	97	93	27	2.1
***m*-III**$_{a}$	107	105	10	2.7
***m*-III**$_{b}$	103	100	14	2.6
***m*-III**$_{c}$	107	102	14	2.4
***m*-III**$_{d}$	104	100	17	2.5
***m*-III**$_{e}$	–	103	9	2.4
***m*-III**$_{f}$	–	105	9	2.3
***m*-III**$_{g}$	–	97	9	2.2
***m*-III**$_{h}$	103	102	12	2.2
***m*-III**$_{i}$	101	99	10	2.3
***m*-III**$_{j}$	102	98	11	2.2

[a] The films were cast from slow evaporation of polymer solutions of DMAc

Table 5 Thermal behavior data of poly(amide–imide)s

Polymer	Differential scanning calorimetry T_g (°C)[a]	Thermogravimetric analysis		
		Decomposition temperature (°C)[b]		Wt% residue at 800 °C in N_2
		In N_2	In air	
***p*-III**$_{a}$	–	527	533	55
***p*-III**$_{b}$	–	529	532	60
***p*-III**$_{c}$	322	540	529	56
***p*-III**$_{d}$	–	509	514	56
***p*-III**$_{e}$	303	540	523	57
***p*-III**$_{f}$	286	537	530	57
***p*-III**$_{g}$	281	537	526	57
***p*-III**$_{h}$	317	546	531	58
***p*-III**$_{i}$	281	525	513	56
***p*-III**$_{j}$	293	539	532	55
***m*-III**$_{a}$	311	547	535	55
***m*-III**$_{b}$	324	553	542	59
***m*-III**$_{c}$	298	547	533	57
***m*-III**$_{d}$	328	533	530	59
***m*-III**$_{e}$	283	546	531	59
***m*-III**$_{f}$	264	544	537	59
***m*-III**$_{g}$	265	536	531	59
***m*-III**$_{h}$	280	552	546	62
***m*-III**$_{i}$	259	521	518	57
***m*-III**$_{j}$	266	532	530	55

[a] Baseline shift in the second heating differential scanning calorimetry traces, with a heating rate of 15 °C/min

[b] Temperatures at which 10% weight loss were recorded by thermogravimetric analysis at a heating rate of 20 °C/min

is much smaller than –CF_3. Therefore, ***p*-III$_j$** and ***m*-III$_j$** based on **II$_j$** had increased steric hindrances, so their polymer chains rotated at higher temperature. Polymers ***p*-III$_e$** and ***m*-III$_e$**, whose diamine structures are all para-oriented, showed higher T_g values than ***p*-III$_{f,g}$** and ***m*-III$_{f,g}$**, derived from meta- or ortho-oriented diamines. The reason is that the meta- or ortho-position substituent increases the intermolecular free volumes such that the polymer chains are easy to rotate. As a whole, series ***p*-III** exhibited obviously higher T_g values than series ***m*-III**, because series ***p*-III** contained more *p*-phenylene groups in the polymer chains.

The thermal stability of these poly(amide–imide)s was characterized by TG analysis conducted at a heating rate of 20 °C/min. The temperatures of 10% weight loss (T_{10}) in nitrogen and air atmospheres were determined from original thermograms and are also tabulated in Table 5. The T_{10} values of these polymers stayed in the range 509–552 °C in nitrogen and in the range 513–546 °C in air, respectively. The lowest thermal stability of ***p*-III$_i$** and ***m*-III$_i$** was brought about by the easy degradation of the aliphatic isopropane group on heating. By comparison of the diamines, ***p*-III$_j$** and ***m*-III$_j$** had better thermal stability than analogous ***p*-III$_i$** and ***m*-III$_i$** because the C–F bond energy of the CF_3 group is larger than the C–H bond energy of the CH_3 group. Generally speaking, the polymers exhibited good thermal stability with no significant weight loss up to approximately 450 °C in both air and nitrogen atmospheres, and the anaerobic char yield was above 55%, showing a high intrinsic fire resistance.

Conclusion

Most of the common polyimides or poly(amide–imide)s have an intense color and are insoluble in organic solvents. In this study, two kinds of isomeric diacid monomers ***p*-I** and ***m*-I**, which contain hexafluoroisopropylidene linking group, were successfully synthesized, and two series of poly(amide–imide)s were synthesized with various aromatic diamines. These poly(amide–imide)s have good solubilities, especially they exhibit better solubilities in less polar solvents than common poly(amide–imide)s. They can be cast into transparent, tough films with DMAc as a solvent. The films were light in color and highly transparency, and they were lighter in color than other similar polymers. Besides, these polymers were characterized by excellent thermal stability together with good tensile properties. Thus, these polymers demonstrate a good combination of physical properties and optical transparency, and they are considered as new candidates for processable high-performance polymeric materials.

Acknowledgement The authors are grateful to the National Science Council of the Republic of China for the support of this work (grant NSC 89-2218-E-036-015).

References

1. Feger C, Khojasteh MM, Htoo MS (1993) Advances in polyimide science and technology. Technomic, Lancaster
2. Adadie MJM, Sillion B (1991) Polyimides and other high-temperature polymers. Elsevier, Amsterdam
3. Mittal KL (1984) Polyimide: synthesis, characterization, and application, vols 1 and 2. Plemnum, New York
4. Feger C, Khojasteh MM, McGrath JE (1989) Polyimides, chemistry and characterization. Elsevier, Amsterdam
5. Wilson D, Stenzenberger HD, Hergenrother PM (1990) Polyimides. Black and Son, Glasgow
6. Cassidy PE (1980) Thermally stable polymers. Dekker, New York
7. Ghosh MK, Mittal KL (1996) Polyimides: fundamentals and applications. Dekker, New York
8. (a) Dupont BS, Bilow N (1986) US Patent 4,592,925; (b) Landis AL, Naselow AB (1987) US Patent 4,645,824
9. (a) Higashi K, Noda Y (1986) Eur Patent 240249; (b) Tamai S, Ohta M, Kawashima S, Oikawa H, Ohkoshi K, Yamaguchi A (1987) Eur Patent 234882
10. Matsuura T, Ando S, Sasaki S, Yamamoto F (1993) Electron Lett 29:2107
11. Ando S, Sawada T, Inoue Y (1993) Electron Lett 29:2143
12. Rogers FE (1964) US Patent 3,356, 648
13. Dine-Hart RA, Wright WW (1971) Makromol Chem 143:189
14. St Clair AK, St Clair TL, Shevket KI (1984) Polym Mater Sci Eng 51:62
15. St Clair AK, St Clair TL, Slemp WS, Ezzell KS (1985) Proceedings of the 2nd international conference on polyimides, Ellenville, New York, p 333
16. Jin Q, Yamashita T, Horie K (1994) J Polym Sci Part A Polym Chem 31:503
17. Yang CP, Hsiao SH (1989) Makromol Chem 190:2119
18. Yang CP, Hsiao SH, Lin JH (1992) Makromol Chem 193:445
19. Yang CP, Chen RS, Chen HD (1999) Polym J 31:1253
20. Yang CP, Chen RS, Chen JA (2000) J Polym Sci Part A Polym Chem 38:1
21. Chen JA, Yang CP (2000) J Appl Polym Sci 77:217
22. Yang CP, Chen RS, Chang CC (2000) Colloid Polym Sci 278:1043
23. Yang CP, Chen RS (1999) Polymer 40:1025
24. Yang CP, Chen RS, Huang CC (1999) J Polym Sci Part A Polym Chem 37:2421
25. Bruma M, Schulz B, Mercer FW (1994) Polymer 35:4209
26. Bruma M, Mercer FW, Fitch JW III, Cassidy PE (1995) J Appl Polym Sci 56:527
27. Irvin DJ, Cassidy PE, Cameron ML (1990) Electron Mater 4:223
28. Irvin DJ, Cassidy PE, Meurer DL, Fitch III JW, Taylor DA (1996) Polymer 37:2227
29. Hamciuc C, Bruma M, Mercer FW, Kopnick T, Schulz B (2000) Macromol Mater Eng 276/277:38
30. Liaw DJ, Liaw BY, Tseng JM (1999) J Polym Sci Part A Polym Chem 37:2629
31. Hsiao SH, Yang CP, Chen SH (2000) J Polym Sci Part A Polym Chem 38:1551
32. Ando S, Matsuura T, Sasaki S (1997) Polym J 29:69